STRUCTURAL CHEMISTRY

ISSN 2053-2296

Protonated oxalyl chloride and the $ClCO^+$ cation

Sebastian Steiner,* Kristina Djordjevic, Valentin Bockmair, Dirk Hollenwäger and Andreas J. Kornath‡

Department Chemie, Ludwig-Maximilians Universität, Butenandtstrasse 5-13 (Haus D), D-81377 München, Germany.
*Correspondence e-mail: sebastian.steiner@cup.uni-muenchen.de

Received 23 September 2024
Accepted 5 November 2024

Edited by M. Yousufuddin, University of North Texas at Dallas, USA

‡ Deceased

Keywords: oxalyl chloride; chlorocarbonyl cation; superacid; protonation; structure elucidation; crystal structure.

CCDC references: 2304793; 2304777

Supporting information: this article has supporting information at journals.iucr.org/c

The reactions of oxalyl chloride were investigated in the binary superacidic systems HF/SbF_5 and DF/SbF_5. *O*-Monoprotonated oxalyl chloride was isolated and represents the first example of a protonated acyl chloride. Diprotonated oxalyl chloride is only stable in solution. Salts of the $ClCO^+$ cation were synthesized from the reactions of oxalyl chloride or COClF with SbF_5 in 1,1,1,2-tetrafluoroethane (R-134a, CF_3CFH_2). The colourless salts were characterized by low-temperature vibrational spectroscopy, NMR spectroscopy and single-crystal X-ray diffraction. (1,2-Dichloro-2-oxoethylidene)oxidanium hexafluoridoantimonate(V), $[C_2O(OH)Cl_2][SbF_6]$, crystallizes in the monoclinic space group $P2_1$ and carbonyl chloride hexadecafluoridotriarsenate(V) $[ClCO][Sb_3F_{16}]$, in the trigonal space group $P3_1$, with two and three formula units per unit cell, respectively. Monoprotonated oxalyl chloride and the $ClCO^+$ cation both display very short C—Cl bonds with a strong double-bond character.

1. Introduction

Oxalyl chloride was first prepared by Fauconnier in 1892 by the reaction of diethyl oxalate and phosphorus pentachloride (Fauconnier, 1892). Nowadays, it is commercially produced by the photochlorination of ethylene carbonate (Pfoertner & Oppenländer, 2012). Due to its high reactivity, oxalyl chloride is one of the most versatile organic reagents in chemical syntheses. Among others, it is used in chlorinations, oxidations, reductions, dehydrations, decarboxylations or formylation reactions (Masaki & Fukui, 1977; Omura & Swern, 1978; Shiri & Kazemi, 2017; Denton *et al.*, 2012; Wasserman & Tremper, 1977; Mendelson & Hayden, 1996). The best-known applications are its use in Friedel–Crafts reactions (Alexandrou, 1969; Ketcha & Gribble, 1985) or the Swern oxidation, *i.e.* the oxidation of primary and secondary alcohols to aldehydes and ketones (Omura & Swern, 1978).

The reactivity of oxalyl chloride towards strong Lewis acids has been thoroughly investigated. Thus, the chlorocarbonyl cation ($ClCO^+$) is observed in the reaction of oxalyl chloride with SbF_5 (Prakash *et al.*, 1991). The $ClCO^+$ cation is a representative of the compound class of linear triatomic molecules, such as OCS, ONP or ONS^+, for which numerous theoretical calculations have been performed (Peterson *et al.*, 1991; Pak & Woods, 1997). It can be synthesized by reacting SbF_5 with either oxalyl chloride, phosgene or carbonyl chloride fluoride. Furthermore, the reaction of carbon monoxide with chlorine in SO_2ClF/SbF_5 leads to the formation of the $ClCO^+$ cation (Prakash *et al.*, 1991; Bernhardt *et al.*, 1999; Christe *et al.*, 1999). The latter was investigated by Olah in 1991 using NMR spectroscopy (Prakash *et al.*, 1991), while Aubke characterized the species by Raman and IR spectroscopy for the first time in 1999 (Bernhardt *et al.*, 1999).

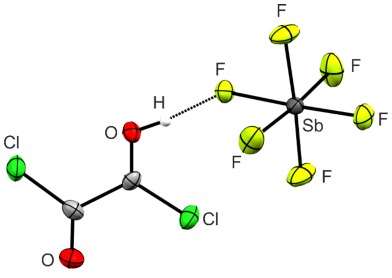

However, it has not yet been possible to elucidate the crystal structure of the cation due to its high reactivity. This prompted us to isolate the $ClCO^+$ cation and to perform single-crystal X-ray diffraction analysis to structurally characterize the cation and to compare its bond lengths with isoelectronic molecules such as OCS, which shows a short C—S bond with a strong C═S double-bond character (Pak & Woods, 1997).

Furthermore, in previous studies by our group, mono- and diprotonated species of oxalic acid, pyruvic acid and parabanic acid were isolated and characterized, whereas the dications constitute vicinal superelectrophiles (Schickinger *et al.*, 2018; Virmani *et al.*, 2022; Beck *et al.*, 2020). In addition, we recently investigated the reactivity of haloacetyl fluorides in superacidic media and observed the protonation of the carbonyl bond, as well as HF addition to the latter, as in the case of dichloroacetyl fluoride (Steiner *et al.*, 2022, 2024). This prompted us to perform investigations on the reactivity of oxalyl chloride in the superacidic system HF/SbF_5.

2. Results and discussion

2.1. Syntheses and properties of $[C_2O(OX)Cl_2][SbF_6]$ (X = H or D), $[C_2(OH)_2Cl_2][Sb_nF_{5n+1}]_2$, $[ClCO][Sb_3F_{15}Cl]$ and $[ClCO][Sb_3F_{16}]$

Oxalyl chloride was reacted in the binary superacidic systems HF/SbF_5 and DF/SbF_5. According to reaction (1) in Scheme 1, $[C_2O(OH)Cl_2][SbF_6]$ (**1**) and $[C_2O(OD)Cl_2][SbF_6]$ (**2**) were obtained as *O*-monoprotonated species of oxalyl chloride in quantitative yields as colourless solids.

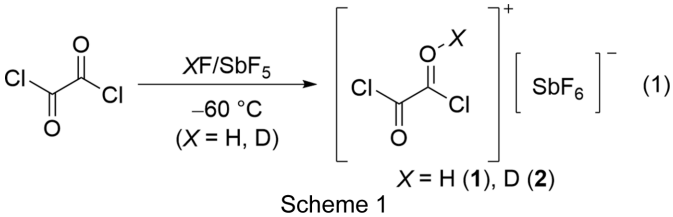

Scheme 1

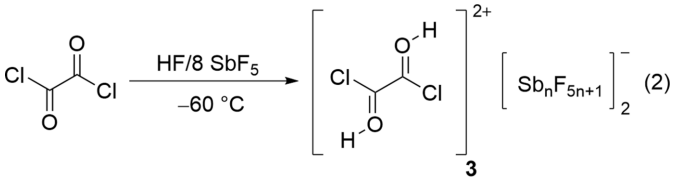

Scheme 2

To obtain the diprotonated species, oxalyl chloride was reacted in the binary superacidic system HF/SbF_5 with an excess of the strong Lewis acid SbF_5. However, even with a tenfold excess of SbF_5, the isolation of diprotonated oxalyl chloride (**3**) as a solid was not possible. Instead of the desired species, monoprotonated oxalyl chloride (**1**) was obtained. To investigate the reaction of oxalyl chloride in anhydrous hydrogen fluoride (aHF) at −60 °C with an excess of SbF_5, NMR spectroscopy was performed employing eight equivalents of SbF_5. Accordingly, the measured ^1H, ^{19}F and ^{13}C NMR spectra indicate the presence of **3** in the solution, as presented in reaction (2) in Scheme 2. Salts **1** and **2** show thermal decomposition at −45 °C.

$[ClCO][Sb_3F_{15}Cl]$ (**4**) was synthesized by reacting oxalyl chloride with three equivalents of SbF_5 in 1,1,1,2-tetrafluoroethane (R-134a, CF_3CFH_2) at −78 °C. **4** was obtained as a colourless solid according to reaction (3) in Scheme 3. To avoid mixed occupancies of the fluorine positions of the anion with chlorine, carbonyl chloride fluoride was reacted under the same conditions to form $[ClCO][Sb_3F_{16}]$ (**5**), as presented in reaction (4) in Scheme 3 (Prakash *et al.*, 1991; Bernhardt *et al.*, 1999; Christe *et al.*, 1999).

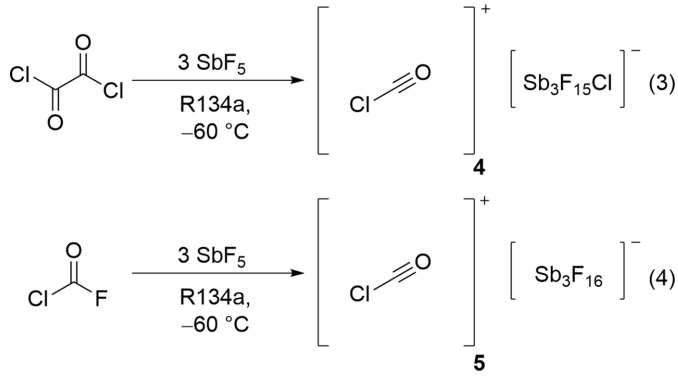

Scheme 3

2.2. Vibrational spectroscopy

The low-temperature Raman (Ra) and infrared (IR) spectra of $[C_2O(OH)Cl_2][SbF_6]$ (**1**), $[C_2O(OD)Cl_2][SbF_6]$ (**2**) and $C_2O_2Cl_2$ are illustrated in Fig. 1. The complete vibrational frequencies of **1**, **2**, **4** and **5**, as well as of oxalyl chloride and carbonyl chloride fluoride, are provided in the supporting information (see Figs. S1–S3 and Tables S1–S5) (Bernhardt *et al.*, 1999; Davis *et al.*, 1993; Nielsen *et al.*, 1952).

For the $[C_2O(OH)Cl_2]^+$ cation with C_s symmetry, 15 fundamental vibrational modes are expected, all of which are Raman and IR active. ν_s(O—H) is superposed by condensed water in the IR spectra due to the measuring method. Furthermore, the O—H stretching vibration shows low intensity in the Raman spectra due to the poor polarizability of the O—H group, which does not apply to the O—D group. The O—D stretching vibration of the D-isotopomeric species **2** is observed at 2157 cm^{-1} in the Raman spectrum and at 2388 cm^{-1} in the IR spectrum. The C═O stretching vibration of the protonated COCl moiety is detected at 1607 cm^{-1} (Ra) (**1** and **2**), as well as at 1605 (**1**) and 1593 cm^{-1} (**2**) (IR), and is significantly red-shifted (by approximately 165 cm^{-1}) compared to the starting material. The vibrations are red-shifted by around 100–150 cm^{-1} in comparison to the corresponding vibrations of protonated acyl fluorides (Steiner *et al.*, 2022, 2024; Bayer *et al.*, 2022). The ν_s(C═O) of the adjacent unprotonated carbonyl group is not affected by the protonation. The C—Cl stretching vibration of the protonated COCl moiety appears at 817 cm^{-1} (**2**) in the Raman spectrum and at 833 cm^{-1} (**1**), as well as at 818 cm^{-1} (**2**), in the IR spectrum,

Table 1
Experimental details.

Experiments were carried out with Mo $K\alpha$ radiation using a Rigaku Xcalibur Sapphire3 diffractometer. Absorption was corrected for by multi-scan methods (*CrysAlis PRO*; Rigaku OD, 2020).

	1	**5**
Crystal data		
Chemical formula	$(C_2HCl_2O_2)[SbF_6]$	$(CClO)[Sb_3F_{16}]$
M_r	363.68	732.71
Crystal system, space group	Monoclinic, $P2_1$	Trigonal, $P3_1$
Temperature (K)	106	102
a, b, c (Å)	6.1616 (8), 10.8379 (10), 6.8805 (8)	8.0824 (3), 8.0824 (3), 18.3341 (8)
α, β, γ (°)	90, 106.472 (13), 90	90, 90, 120
V (Å^3)	440.61 (9)	1037.22 (9)
Z	2	3
μ (mm^{-1})	3.80	6.19
Crystal size (mm)	0.31 × 0.17 × 0.12	0.19 × 0.14 × 0.11
Data collection		
T_{min}, T_{max}	0.737, 1.000	0.882, 1.000
No. of measured, independent and observed [$I > 2\sigma(I)$] reflections	8919, 2930, 2692	6310, 3334, 3029
R_{int}	0.042	0.044
$(\sin \theta/\lambda)_{max}$ (Å^{-1})	0.755	0.746
Refinement		
$R[F^2 > 2\sigma(F^2)]$, $wR(F^2)$, S	0.030, 0.057, 1.04	0.038, 0.077, 1.03
No. of reflections	2930	3334
No. of parameters	122	199
No. of restraints	2	0
H-atom treatment	Only H-atom coordinates refined	–
$\Delta\rho_{max}$, $\Delta\rho_{min}$ (e Å^{-3})	1.18, −0.66	1.36, −1.09
Absolute structure	Refined as an inversion twin	Twinning involves inversion, so Flack parameter cannot be determined
Absolute structure parameter	0.52 (3)	–

Computer programs: *CrysAlis PRO* (Rigaku OD, 2020), *SHELXT* (Sheldrick, 2015*a*), *SHELXL2019* (Sheldrick, 2015*b*), *ORTEP-3 for Windows* (Farrugia, 2012) and *PLATON* (Spek, 2020).

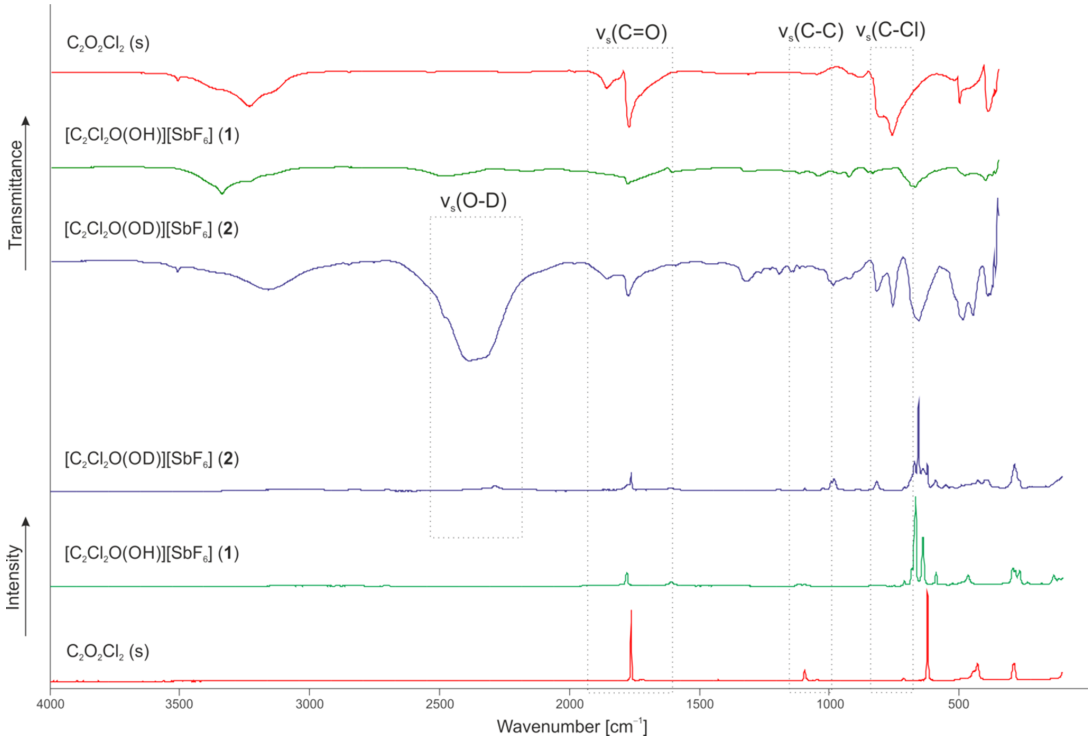

Figure 1
Low-temperature Raman (bottom) and IR spectra (top) of $[C_2O(OX)Cl_2][SbF_6]$ (**1** and **2**) (X = H or D) and $C_2O_2Cl_2$.

i.e. blue-shifted by approximately 70 cm^{-1}. The ν_s(C—Cl) of the neighboring COCl moiety is not affected by protonation and occurs at 623 cm^{-1} (**2**) in the Raman spectrum. Additionally, the C—C stretching vibration is detected at 1118 (Ra) (**1**) and 1117 cm^{-1} (**1** and **2**) (IR), and is thus blue-shifted by approximately 20 cm^{-1} in comparison to oxalyl chloride.

More vibrations are observed for the $[SbF_6]^-$ anion than expected for ideal octahedral symmetry due to interionic interactions in the solid leading to a symmetry distortion (Weidlein *et al.*, 1988).

2.3. Crystal structure of $[C_2O(OH)Cl_2][SbF_6]$ (1)

The hexafluoridoantimonate of monoprotonated oxalyl chloride (**1**) crystallizes in the monoclinic space group $P2_1$ with two formula units per unit cell. The asymmetric unit is illustrated in Fig. 2. Crystal data and structure refinement details are provided in Table 1 and in the supporting information (Tables S6 and S7).

Due to the protonation, the C1—O1 bond length [1.225 (8) Å] is significantly elongated compared to the starting material [1.180 (2) Å; Danielson *et al.*, 1995] and is longer than a formal C═O bond (1.18 Å; Allen *et al.*, 1987). The C2—O2 bond length [1.184 (8) Å] of the adjacent unprotonated C═O bond is not affected by the protonation [1.180 (2) Å; Danielson *et al.*, 1995]. Furthermore, the C1—Cl1 bond length [1.647 (7) Å] is significantly shortened compared to the neutral compound [1.747 (3) Å; Danielson *et al.*, 1995] and is in the range between a formal C—Cl single bond (1.76 Å; Allen *et al.*, 1987) and a C═Cl double bond (1.56 Å; Holleman *et al.*, 1987). The same applies for the C2—Cl2 bond length [1.693 (7) Å] [*cf.* 1.747 (3) Å for oxalyl chloride; Danielson *et al.*, 1995]. The elongation of the C═O bond and the shortening of the C—Cl bonds are consistent with the observed shifts of the ν_s(C═O) and ν_s(C—Cl) in the vibrational spectra. The C1—C2 bond length [1.550 (8) Å] is not affected by protonation [*cf.* 1.545 (8) Å for oxalyl chloride; Danielson *et al.*, 1995]. This is consistent with the results observed for the mono- and diprotonated species of oxalic acid. In both cases, the protonation at the carbonyl groups does not affect the bond lengths of the C—C backbone (Schickinger *et al.*, 2018).

The Sb—F bond lengths are in the range between 1.846 (4) and 1.941 (3) Å, and correspond with values reported in the literature (Minkwitz *et al.*, 1999*a*,*b*; Minkwitz & Schneider, 1999). Due to interionic interactions, the anion displays distorted octahedral symmetry. The Sb1—F6 bond [1.941 (3) Å] is significantly longer than the other Sb—F bonds with it being involved in hydrogen bonding.

In the crystal structure of **1**, the ions are arranged into chains along the *a* and *b* axes by the strong O1(—H1)···F6 hydrogen bond [2.421 (7) Å] and the C···F interactions C1···F2^{i} [2.617 (7) Å; see Fig. 4 for symmetry codes] and C1···F4^{ii} [2.565 (7) Å] (see Figs. S4–S5) (Jeffrey, 1997; Bondi, 1964). The chains are linked to each other by the Cl···F interaction Cl1···F3^{iii} [2.883 (5) Å] to form layers. All interatomic C···F and Cl···F contacts are below the sum of the van der Waals radii (3.17 and 3.22 Å; Bondi, 1964). Interatomic distances are listed in Table S7.

2.4. Crystal structure of $[ClCO][Sb_3F_{16}]$ (5)

The crystal structures of **4** and **5** were both obtained by recrystallizing the salts from R-134a (CF_3CFH_2) at −40 °C. As **4** crystallizes as an inversion twin and shows mixed occupancies of all 16 crystallographic fluorine positions with chlorine, the structural parameters show high standard deviations. Therefore, the crystal structure of **5** is used for the discussion of all experimental parameters.

$[ClCO][Sb_3F_{16}]$ (**5**) crystallizes in the trigonal space group $P3_1$ with three formula units per unit cell. The asymmetric unit is depicted in Fig. 3. Crystal data and structure refinement details are provided in Table 1 and in the supporting information (Tables S6 and S8).

The C1—O1 bond length [1.105 (10) Å] is significantly shortened compared to ClFCO [1.173 (2) Å; Oberhammer, 1980]. It is in the range between a formal C═O double bond (1.19 Å) and a C≡O triple bond (1.07 Å) (Allen *et al.*, 1987). It corresponds with the C═O bond length (1.1562 Å) of the

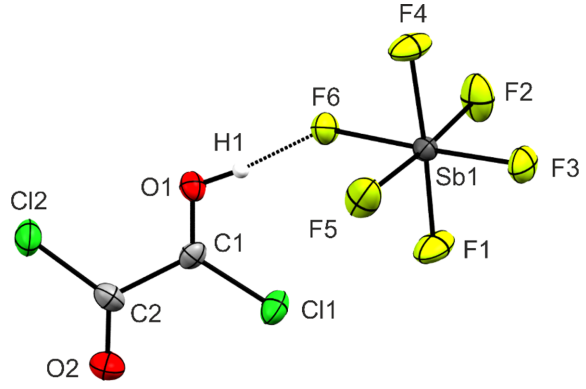

Figure 2
The asymmetric unit of **1**, with displacement ellipsoids drawn at the 50% probability level.

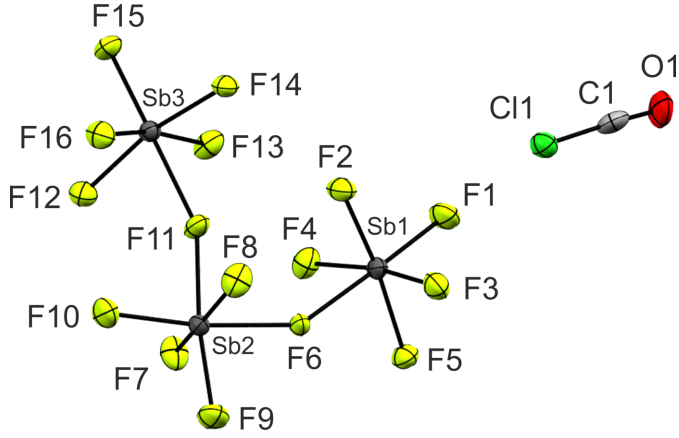

Figure 3
The asymmetric unit of **5**, with displacement ellipsoids drawn at the 50% probability level.

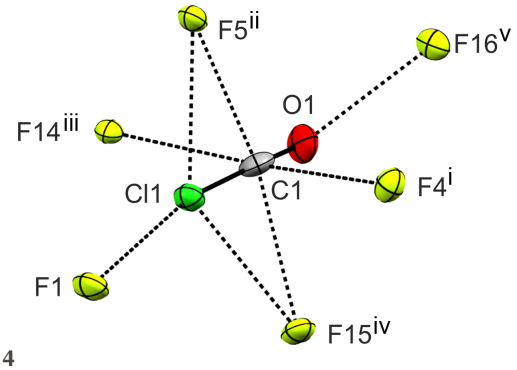

Figure 4
Interatomic contacts of **5**, with displacement ellipsoids drawn at the 50% probability level. [Symmetry codes: (i) $x-1, y, z$; (ii) $-x+y, -x+1, z-\frac{1}{3}$; (iii) $x, y+1, z$; (iv) $-y, x-y, z+\frac{1}{3}$; (v) $x-1, y+1, z$.

isoelectronic molecule OCS (Pak & Woods, 1997). Furthermore, the C1—Cl1 bond length [1.571 (3) Å] is significantly shortened compared to ClFCO [1.725 (2) Å; Oberhammer, 1980]. It is in the range of a formal C═Cl double-bond length (1.56 Å) and thus displays a significant double-bond character (Allen *et al.*, 1987). It corresponds with the C—Cl bond length [1.67 (2) Å] of ClCN (Beach & Turkevich, 1939). The Cl1—C1—O1 angle [176.1 (8)°] indicates the essentially linear structure of the cation.

The Sb—F bond lengths of the terminal F atoms are in the range between 1.831 (8) and 1.857 (7) Å. The bridging Sb—F bonds are longer than the terminal ones, with bond lengths up to 2.088 (8) Å. The bond angles Sb1—F6—Sb2 [146.0 (4)°] and Sb2—F11—Sb3 [156.6 (4)°] are also in good agreement with the literature (Faggiani *et al.*, 1986; Gerken *et al.*, 2002).

In the crystal structure of **5**, the ions form a helical structure along the *c* axis *via* the C···F interaction C1···F5^{ii} (2.75 Å) and the Cl···F interaction Cl1···F1 [2.56 (1) Å] (see Fig. 4, and Figs. S6–S7 in the supporting information). The cation displays a tetracoordinated C1 atom and further forms the interionic contacts C1···F4^{i} (2.968 Å), C1···F14^{iii} (3.062 Å), C1···F15^{iv} (2.92 Å) and O1···F16^{v} [2.79 (2) Å] (see Fig. 4). All interatomic C···F, Cl···F and O···F contacts are below the sum of the van der Waals radii (3.17, 3.22 and 2.99 Å; Bondi, 1964). Selected interatomic distances are listed in Table S8.

2.5. NMR spectroscopy

To trace the reactivity of oxalyl chloride in aHF and the binary superacidic system HF/SbF_5, the ^{1}H, ^{19}F and ^{13}C NMR spectra were measured at −60 °C with acetone-d_6 as the external standard. The measured NMR spectra and the complete NMR data of oxalyl chloride, **1** and **3** are listed in the supporting information (Figs. S8–S18).

The ^{13}C NMR spectrum of oxalyl chloride dissolved in aHF at −60 °C shows a singlet at 161.1 ppm for both COCl moieties. Furthermore, no chlorine–fluorine exchange or HF addition to the carbonyl bond is observed under these conditions.

By first dissolving equimolar amounts of SbF_5 compared to oxalyl chloride in HF and then adding the acyl chloride, monoprotonated oxalyl chloride (**1**) is formed. The ^{1}H NMR spectrum shows a singlet at 10.03 ppm for the protonated carbonyl group. The ^{13}C NMR spectrum displays two singlets located at 161.7 and 183.4 ppm. These are assigned to the carbonyl groups, whereas the NMR resonance of the protonated COCl moiety is significantly shifted downfield. The ^{19}F NMR spectrum indicates chlorine–fluorine exchange initiated by the protonation of oxalyl chloride. Thus, the NMR resonance at 17.74 ppm indicates the formation of oxalyl fluoride. The ^{1}H, ^{19}F and ^{13}C NMR spectra of $(COF)_2$ at −60 °C in aHF are illustrated in Figs. S10–S11 (see supporting information). Furthermore, in the ^{19}F NMR spectrum, the resonance at −124.78 ppm is assigned to the $[SbF_6]^-$ anion (Dean & Gillespie, 1969).

Since the diprotonated oxalyl chloride (**3**) could not be isolated as a solid, the reaction of oxalyl chloride in HF/SbF_5 at −60 °C was investigated using NMR spectroscopy, whereas an eightfold amount of SbF_5 was applied. Accordingly, the NMR spectra indicate the presence of **3** in the solution. The ^{1}H NMR spectrum shows a singlet at 9.61 ppm for the protonated $COCl^+$ moieties, whereas the ^{13}C NMR spectrum displays a singlet at 183.1 ppm. Compared to the neutral compound, the ^{13}C NMR resonance is significantly shifted downfield. Furthermore, in the ^{19}F NMR spectrum, multiple resonances located in the range between −117.46 and −143.05 ppm are assigned to the $[Sb_nF_{5n+1}]^-$ polyanions (Dean & Gillespie, 1969). Thus, diprotonated oxalyl chloride is stable in solution at −60 °C. However, after removal of the excess HF at −78 °C, it decomposes with the formation of **1**. Furthermore, as in the NMR spectra of **1**, a chlorine–fluorine exchange is observed, as the signal at 17.46 ppm indicates the formation of oxalyl fluoride. Additional signals in the ^{19}F NMR spectra of **3** at −21.78 and −59.90 ppm are assigned to COF_2 and CF_3OH (Christe *et al.*, 2007). The ^{1}H, ^{19}F and ^{13}C NMR spectra of COF_2 in aHF at −60 °C are depicted in the supporting information (Fig. S12). COF_2 is likely formed due to the decomposition of oxalyl fluoride under superacidic conditions.

3. Conclusions

Oxalyl chloride was reacted in the binary superacidic systems HF/SbF_5 and DF/SbF_5 to form the *O*-monoprotonated and its D-isotopomeric species as hexafluoridoantimonates. Both represent the first examples of protonated acyl chlorides. When the Lewis acid SbF_5 is applied in eightfold excess, diprotonated oxalyl chloride is formed, which is only stable in solution. By the reaction of oxalyl chloride or carbonyl chloride fluoride in the aprotic solvent 1,1,1,2-tetrafluoroethane (R-134a, CF_3CFH_2) with a threefold excess of SbF_5, salts of the chlorocarbonyl cation were isolated. The colourless salts were characterized by low-temperature vibrational spectroscopy and low-temperature NMR spectroscopy. The crystal structures of $[C_2O(OH)Cl_2][SbF_6]$ and $[ClCO][Sb_3F_{16}]$ were determined by single-crystal X-ray diffraction analysis.

Monoprotonated oxalyl chloride and the chlorocarbonyl cation both display very short C—Cl bonds with strong double-bond character.

Acknowledgements

We are grateful to the Department of Chemistry of the Ludwig Maximilian University, the Deutsche Forschungsgemeinschaft (DFG) and F-Select GmbH for the financial support of this work. Special thanks go to Professor Dr Konstantin Karaghiosoff for help with this work after Professor Dr Andreas J. Kornath passed away. Open access funding enabled and organized by Projekt DEAL.

References

Alexandrou, N. E. (1969). *J. Chem. Soc. C*, pp. 536–537.
Allen, F. H., Kennard, O., Watson, D. G., Brammer, L., Orpen, A. G. & Taylor, R. (1987). *J. Chem. Soc. Perkin Trans. 2*, pp. S1–S19.
Bayer, M. C., Kremser, C., Jessen, C., Nitzer, A. & Kornath, A. J. (2022). *Chem. A Eur. J.* **28**, e202104422.
Beach, J. Y. & Turkevich, A. (1939). *J. Am. Chem. Soc.* **61**, 299–303.
Beck, S., Raljic, M., Jessen, C. & Kornath, A. J. (2020). *Eur. J. Org. Chem.* **2020**, 4521–4527.
Bernhardt, E., Willner, H. & Aubke, F. (1999). *Angew. Chem. Int. Ed.* **38**, 823–825.
Bondi, A. (1964). *J. Phys. Chem.* **68**, 441–451.
Christe, K. O., Hegge, J., Hoge, B. & Haiges, R. (2007). *Angew. Chem. Int. Ed.* **46**, 6155–6158.
Christe, K. O., Hoge, B., Boatz, J. A., Prakash, G. K. S., Olah, G. A. & Sheehy, J. A. (1999). *Inorg. Chem.* **38**, 3132–3142.
Danielson, D. D., Hedberg, L., Hedberg, K., Hagen, K. & Trtteberg, M. (1995). *J. Phys. Chem.* **99**, 9374–9379.
Davis, J. F., Wang, A. & Durig, J. R. (1993). *J. Mol. Struct.* **293**, 27–30.
Dean, P. A. W. & Gillespie, R. J. (1969). *J. Am. Chem. Soc.* **91**, 7260–7264.
Denton, R. M., An, J., Lindovska, P. & Lewis, W. (2012). *Tetrahedron*, **68**, 2899–2905.
Faggiani, R., Kennepohl, D. K., Lock, C. J. L. & Schrobilgen, G. J. (1986). *Inorg. Chem.* **25**, 563–571.
Farrugia, L. J. (2012). *J. Appl. Cryst.* **45**, 849–854.
Fauconnier, A. (1892). *C. R. Acad. Sci.* **114**, 122–123.
Gerken, M., Dixon, D. A. & Schrobilgen, G. J. (2002). *Inorg. Chem.* **41**, 259–277.
Holleman, A. F., Wiberg, E. & Wiberg, N. (2017). In *Anorganische Chemie*. Berlin, Boston: De Gruyter.
Jeffrey, G. A. (1997). In *An Introduction to Hydrogen Bonding: Topics in Physical Chemistry*. New York: Oxford University Press Inc.
Ketcha, D. M. & Gribble, G. W. (1985). *J. Org. Chem.* **50**, 5451–5457.
Masaki, M. & Fukui, K. (1977). *Chem. Lett.* **6**, 151–152.
Mendelson, W. L. & Hayden, S. (1996). *Synth. Commun.* **26**, 603–610.
Minkwitz, R., Hartfeld, N. & Hirsch, C. (1999*a*). *Z. Anorg. Allg. Chem.* **625**, 1479–1485.
Minkwitz, R., Hirsch, C. & Berends, T. (1999*b*). *Eur. J. Inorg. Chem.* **1999**, 2249–2254.
Minkwitz, R. & Schneider, S. (1999). *Angew. Chem. Int. Ed.* **38**, 210–212.
Nielsen, A. H., Burke, T. G., Woltz, P. J. H. & Jones, E. A. (1952). *J. Chem. Phys.* **20**, 596–604.
Oberhammer, H. (1980). *J. Chem. Phys.* **73**, 4310–4313.
Omura, K. & Swern, D. (1978). *Tetrahedron*, **34**, 1651–1660.
Pak, Y. & Woods, R. C. (1997). *J. Chem. Phys.* **107**, 5094–5102.
Peterson, K. A., Mayrhofer, R. C. & Woods, R. C. (1991). *J. Chem. Phys.* **94**, 431–441.
Pfoertner, K.-H. & Oppenländer, T. (2012). *Photochemistry. Ullmann's Encyclopedia of Industrial Chemistry*. Weinheim: Wiley-VCH.
Prakash, G. K. S., Bausch, J. W. & Olah, G. A. (1991). *J. Am. Chem. Soc.* **113**, 3203–3205.
Rigaku OD (2020). *CrysAlis PRO*. Rigaku Oxford Diffraction Ltd, Yarnton, Oxfordshire, England.
Schickinger, M., Saal, T., Zischka, F., Axhausen, J., Stierstorfer, K., Morgenstern, Y. & Kornath, A. J. (2018). *ChemistrySelect*, **3**, 12396–12404.
Sheldrick, G. M. (2015*a*). *Acta Cryst.* A**71**, 3–8.
Sheldrick, G. M. (2015*b*). *Acta Cryst.* C**71**, 3–8.
Shiri, L. & Kazemi, M. (2017). *Res. Chem. Intermed.* **43**, 6007–6041.
Spek, A. L. (2020). *Acta Cryst.* E**76**, 1–11.
Steiner, S., Jessen, C. & Kornath, A. J. (2022). *Z. Anorg. Allge Chem.* **648**, e202200060.
Steiner, S., Nitzer, A., Jessen, C. & Kornath, A. J. (2024). *Z. Anorg. Allge Chem.* **650**, e202400013.
Virmani, A., Pfeiffer, M., Jessen, C., Morgenstern, Y. & Kornath, A. J. (2022). *Z. Anorg. Allge Chem.* **648**, e202200005.
Wasserman, H. H. & Tremper, A. W. (1977). *Tetrahedron Lett.* **18**, 1449–1450.
Weidlein, J., Müller, U. & Dehnicke, K. (1988). In *Schwingungsspektroskopie. Eine Einführung*. Stuttgart: Thieme.

supporting information